^{18}F α-Methyl Tyrosine PET Studies in Patients with Brain Tumors

Tomio Inoue, Takashi Shibasaki, Noboru Oriuchi, Keiko Aoyagi, Katsumi Tomiyoshi, Shigeko Amano, Masahiko Mikuni, Itsurou Ida, Jun Aoki and Keigo Endo

Departments of Nuclear Medicine, Neurosurgery, Diagnostic Radiology and Neuropsychiatry, Gunma University School of Medicine, Gunma, Japan

We have developed ^{18}F-labeled α-methyl tyrosine (FMT) for PET imaging. The aim of this study was to evaluate the clinical application potential of FMT for patients with brain tumors. **Methods:** Eleven healthy volunteers and 20 patients with brain tumors were injected with 185 MBq (5 mCi) FMT. In 3 healthy volunteers, whole-body imaging and urinary and plasma analysis were conducted for the assessment of the biodistribution of FMT. The normal range of cortical standardized uptake value (SUV) as a reference for comparing tumor SUV of FMT was estimated by using PET data obtained at 30 min postinjection in 8 healthy volunteers. Dynamic PET scans were conducted for 100 min in 4 healthy volunteers and for 30 min in 15 patients with brain tumors. The 10-min static images in another 4 volunteers and all patients were obtained at 30 min postinjection. In 13 patients, FMT uptake in the brain tumor was compared with ^{18}F-fluorodeoxyglucose (FDG). Tumor-to-normal cortex count (T/N) ratio and tumor-to-white matter count (T/W) ratio and SUVs of brain tumors were determined on FMT and FDG PET images. **Results:** Approximately 1480 MBq (40 mCi) FMT were produced in one radiosynthesis. Percentage injected dose (%ID) of FMT in the brain ranged from 2.8% to 4.9%, and approximately 50%ID of FMT was excreted in urine during 60 min postinjection, of which 86.6% was unmetabolized FMT. A faint physiological brain uptake with SUV of 1.61 ± 0.32 (mean ± SD, n = 8) was observed in healthy volunteers. Tumor SUV of FMT ranged from 1.2 to 8.2, with mean value of 2.83 ± 1.57 (n = 23), which was significantly higher than that of the cortical area in healthy volunteers ($P < 0.01$). T/N and T/W ratios of FMT were significantly higher than those of FDG (2.53 ± 1.31 versus 1.32 ± 1.46, $P < 0.001$; 3.99 ± 2.10 versus 1.39 ± 0.65, $P < 0.0001$, respectively). **Conclusion:** FMT, like other radiolabeled amino acids, can provide high-contrast PET images of brain tumors.

Key Words: α-methyl tyrosine; brain tumor; PET

J Nucl Med 1999; 40:399–405

L-[methyl-^{11}C]methionine (^{11}C-MET), an essential amino acid tracer for PET tumor imaging, is proven to be useful in delineating brain tumors (*1*). Many other amino acids have been labeled with ^{11}C (*2–6*). Recently, ^{11}C-choline (*7,8*) and ^{11}C-tyrosine (^{11}C-Tyr) (*9,10*) were also reported as efficient agents for PET tumor imaging in patients with brain tumors. However, the short half-life of 20 min of ^{11}C requires in-house radiosynthesis and repeated radiolabeling for each PET study, resulting in a limited number of PET studies. The glucose analog ^{18}F-fluorodeoxyglucose (FDG) is widely used for detecting various tumors (*11*), and it has a longer physical half-life (109 min) than ^{11}C-labeled agents. Although the detectability of FDG PET for tumors, except brain tumors, is reported to be similar to that of ^{11}C-MET (*12*), the high glucose use of gray matter hampers the identification of brain tumors by FDG PET (*13,14*). To overcome these drawbacks of FDG and ^{11}C-labeled agents, an amino acid tracer with a long half-life of ^{18}F is desirable. From this viewpoint, L-[2–^{18}F]fluorotyrosine (^{18}F-Tyr) (*15*) and L-[2–^{18}F]fluorophenylalanine (^{18}F-Phe) (*16*) have been developed and evaluated as tumor-seeking agents. However, the use of ^{18}F-Tyr and ^{18}F-Phe remains limited because of rather ineffective radiosynthesis. Recently, we developed L-[3–^{18}F]-α-methyl tyrosine (FMT) as a tumor-detecting amino acid tracer for PET imaging (*17*) because L-3-[^{123}I]iodo-α-methyl tyrosine (IMT) was already proven to be clinically useful for SPECT imaging in patients with brain tumors (*18,19*). Because the potential use of FMT as a tumor-detecting agent for PET imaging was confirmed by using experimental tumor models (*20,21*), a preliminary clinical trial of FMT PET for the detection of tumors was undertaken in our institute. The aim of this study was to assess the clinical application potential of FMT for patients with brain tumors.

MATERIALS AND METHODS

Patients

The patients' characteristics, including age, sex, histopathologic features, localization of tumors, pretreatment, interval from the last treatment (if any) to the FMT PET scan, method of verification of FMT PET results, contrast enhancement on CT or MRI and tumor size are listed in Table 1.

Twenty patients with suspected brain tumors (12 females, 8 males; mean age 41 ± 21 y, range 1–71 y) and 11 volunteers (3 women, 8 men; mean age 40 ± 13 y, range 21–60 y) who had undergone FMT PET imaging were included in this study over a 17-mo period. Informed consent was obtained from each patient or child's guardian before the PET study. Twenty patients with brain tumors included the following: 8 patients with low-grade glioma

Received Apr. 4. 1998; revision accepted Jun. 18, 1998.

For correspondence or reprints contact: Tomio Inoue, MD, Department of Nuclear Medicine, Gunma University School of Medicine, 3–39–22 Showa-machi Maebashi, Gunma, 371–8511 Japan.

TABLE 1
Patients' Characteristics and Results of PET with ^{18}F α-Methyl Tyrosine

Patient no.	Age (y)	Sex	Initial histology	Site of disease	Treatment before PET	Time from treatment to PET	Method of verification	MRI/CT	Tumor size (cm)	T/N		T/W		SUV of lesion	
										FMT	FDG	FMT	FDG	FMT	FDG
1	30	M	Astrocytic tumor grade I	Right frontal lobe	OP + IRT	3 y	Surgery	C	2.6	1.42	0.52	1.82	0.89	2.6	ND
2	34	F	Astrocytic tumor grade II	Left frontal lobe	None	—	Surgery	NC	3.0	1.94	0.65	2.85	0.92	2.5	ND
3	1	F	Astrocytic tumor grade II	Suprasellar region	None	—	Surgery	C	4.0	0.96	ND	2.21	ND	1.7	ND
4	52	F	Astrocytic tumor grade II	Right frontal lobe	None	—	Biopsy	NC	2.0	2.14	0.89	6.00	1.03	2.7	ND
5	27	M	Astrocytic tumor grade II	Right frontal lobe	OP	3 y	Surgery	C	8.0	3.37	1.05	5.82	1.23	6.4	3.8
6	32	F	Astrocytic tumor grade II	Left front–parietal lobe	OP + CHE	8 y	Surgery	C	4.0	3.13	0.64	5.00	1.13	2.5	2.7
7	49	M	Astrocytic tumor grade II	Right front–parietal lobe	OP + IRT	8 mo	Follow-up	*	3.5	1.60	ND	2.50	ND	1.5	ND
8	53	M	Astrocytic tumor grade II	Right temporal lobe	OP + IRT	4 y	Follow-up	C	2.3	2.22	ND	2.70	ND	2.3	ND
9	52	F	Astrocytic tumor grade III	Right frontal and temporal lobe	None	—	Surgery	C	4.0	2.63	1.61	3.14	3.31	2.8	5.3
10	60	F	Astrocytic tumor grade III	Right parietal and occipital lobe	None	—	Surgery	C	5.0	6.03	1.15	8.63	1.80	8.2	9.9
11	16	F	Astrocytic tumor grade III	Left cerebellum	OP	18 mo	Follow-up	C	4.5	3.86	ND	6.75	ND	2.7	ND
12A	17	F	Astrocytic tumor grade III	Right frontal lobe	OP	4 y	Surgery	C	4.5	2.78	0.64	3.25	0.93	2.7	1.4
12B	17	F	Astrocytic tumor grade III	Right frontal lobe	OP + IRT + CHE	6 mo	Follow-up	C	2.0	1.69	ND	2.20	ND	1.8	ND
13A	51	F	Astrocytic tumor grade IV	Left frontal lobe	None	—	Surgery	C	4.0	1.83	ND	2.44	ND	2.2	ND
13B	51	F	Astrocytic tumor grade IV	Left basal ganglia	OP + IRT	2 mo	Follow-up	C	2.0	2.45	ND	3.16	ND	1.2	ND
14A	5	F	Presumed glioma	Pons	IRT + CHE	2 mo	Follow-up	C	2.5	1.30	ND	1.58	ND	3.1	ND
14B	5	F	Presumed glioma	Pons, midbrain and right cerebellum	IRT + CHE	10 mo	Follow-up	C	4.0	2.09	ND	3.29	ND	2.3	ND
15	68	F	Presumed benign glioma	Right thalamus	None	—	Follow-up	NC	1.2	1.22	0.79	2.08	1.57	2.0	ND
16	26	M	Lymphoma	Bilateral corona radiata	None	—	Biopsy	C	3.0	1.14	0.69	1.78	1.50	1.6	2.7
17	71	M	Meningioma	Left basal ganglia	None	—	Surgery	C	4.5	3.40	0.88	6.00	1.57	4.8	4.4
18	53	F	Metastatic lesion of colon cancer	Left temporal lobe	None	—	Follow-up	C	2.5	1.68	ND	2.18	ND	1.7	ND
19	57	M	Melanoma	Left parietal lobe	OP + CHE	2 mo	Follow-up	C	2.5	1.67	0.67	2.86	1.05	2.0	6.2
20	58	M	Metastatic lesion of esophageal cancer	Left parietal and occipital	OP	2 y	Follow-up	C	5.0	2.08	0.75	2.60	1.03	2.6	4.8

*Could not be determined.

T/N = tumor-to-normal cortex count ratio; T/W = tumor-to-white matter count ratio; SUV = standardized uptake value; FMT = ^{18}F α-methyl tyrosine; FDG = fluorodeoxyglucose; OP = operation; IRT = radiotherapy; C = contrast enhancement; ND = not done; NC = no contrast enhancement; CHE = chemotherapy.

(astrocytic tumors) (1 grade I and 7 grade II), 5 with high-grade glioma (4 grade III and 1 grade IV), 2 with presumed glioma, 1 with malignant lymphoma, 1 with meningioma, 1 with melanoma and 2 with metastatic tumor (Table 1). Histopathologic diagnosis of brain tumors was based on the revised World Health Organization classification (22). Diagnoses in the following patients were not confirmed histopathologically but were presumed on the basis of the CT or MR images and clinical course, including response to the

treatment with chemotherapy and/or irradiation. Patient 14 had a markedly enhanced mass in the pons on CT that regrew after irradiation and treatment with anticancer drugs. Patient 15 had a well-defined stable mass on CT and MR images in the right thalamus for 6 mo. Patient 18 had histopathologically proven colon cancer and a contrast-enhanced mass in the left temporal lobe on CT scan. Patient 20, in the postoperative status of esophageal cancer, had multiple lung metastases and a contrast-enhanced mass in the left parieto-occipital lobe on T1-weighted images. Although the other 16 patients had histopathologically proven brain tumors, 13 FMT PET scans in 11 patients were conducted after the treatment of brain tumors. Four FMT PET scans were conducted after the treatment of surgery, 6 were conducted after a combination therapy of surgery and irradiation or chemotherapy, 2 after a combination therapy of irradiation and anticancer drugs and 1 after a combination therapy of surgery, chemotherapy and irradiation. The interval from the last treatment to FMT PET scan ranged from 2 mo to 8 y. Results of 12 FMT PET scans in 12 patients were verified histopathologically with stereotactic biopsy or surgical specimens. The verification of final diagnosis of 11 FMT PET scans in 10 patients was based on the response to treatment and the regrowth of tumor for the observation periods of more than 4 mo.

Preparation of FMT and FDG

FMT was produced in our cyclotron facility according to the method developed by Tomiyoshi et al. (*17*). FDG was synthesized according to a modified method of Hamacher et al. (*23*).

PET Studies

PET was performed with a SET 2400W (Shimadzu Corp., Kyoto, Japan) with a 59.5-cm transaxial field of view, 20-cm axial field of view that produces 63 image planes spaced 3.125 mm apart. Transaxial spatial resolution is 4.2 mm full width at half maximum (FWHM) at the center of the field of view and axial resolution is 5.0 mm FWHM.

To assess the biodistribution of FMT, whole-body images, taken using the simultaneous emission-transmission method (*24*), were obtained at 0–35 min, 60–95 min and 210–245 min postinjection in 3 healthy volunteers. Urine was collected for 0–60 min and 60–180 min, and venous blood samples were taken at 5, 30 and 60 min postinjection from the same 3 healthy volunteers. The metabolic stability of FMT in plasma and urine was evaluated by thin-layer chromatography and high-performance liquid chromatography, respectively. By using "S" values reported in *MIRD Pamphlet No. 11* (*25*), the radiation dose to the whole body was estimated.

To perform measured attenuation correction for the clinical trial of FMT PET, transmission scans with an external source of ^{68}Ge were performed before FMT injection. Healthy volunteers and patients fasted for at least 4 h before the FMT PET study. After intravenous injection of 185 MBq (5 mCi) FMT, consecutive dynamic brain scans with a 5- or 10-min interval were conducted for 100 min in 4 healthy volunteers, and for 30 min in 15 patients with brain tumors. The 10-min static images in another 4 volunteers and all patients were obtained at 30 min postinjection.

Venous blood samples in 4 healthy volunteers were taken at 2, 5, 10, 15, 30, 45, 60, 90 and 120 min postinjection, and the level of radioactivity in plasma was measured with an autowell gamma counter.

Regarding FDG PET, patients fasted for at least 4 h and were injected with approximately 200 MBq (5.4 mCi) FDG. Static brain images with FDG were obtained at 50 min postinjection with the simultaneous emission-transmission technique (*24*). FDG PET scans obtained within 1 wk of the date of FMT PET were included in this study.

Quantitative Analysis

A combined filter of a ramp filter with a critical frequency equal to the Nyquist rate (f_{Nyq} = 1.6 cycles/cm) and a Butterworth filter with a 0.312 cycles/cm cutoff frequency was used as a reconstructed filter to produce the transaxial brain images with FMT and FDG.

Attenuation-corrected images with FMT and FDG were reconstructed into 128 × 128 matrices with pixel dimensions of 4.0 mm in-plane and 9.38 mm axially.

With attenuation-corrected images, injected dose of FMT and FDG, patient's body weight and the cross-calibration factors between PET and dose calibrator, functional images of standardized uptake value (SUV) were also produced. SUV was defined as follows:

$$\text{SUV} = \frac{\text{radioactive concentration in tissue or lesion (MBq/g)}}{\text{injected dose (MBq)/patient's body weight (g)}}.$$

For the analysis of normal brain accumulation of FMT, six round regions of interest (ROIs) 1 cm in diameter over cortical region and two ROIs 1 cm in diameter over white matter were placed manually on SUV images of centrum semiovale. Mean values of ROIs were averaged to be defined as the SUV of cortex and white matter in each patient. The time course of FMT uptake in the cortical region and white matter was observed by generating the time-activity curve of mean SUV in 4 healthy volunteers who underwent dynamic PET. Normal SUV of cortical FMT uptake, as a reference of tumor FMT uptake, was determined by using the data of FMT PET obtained at 30 min postinjection in 8 healthy volunteers: the combined results of 4 healthy volunteers who underwent dynamic scanning and those of the other 4 healthy volunteers who underwent static scanning.

For the analysis of tumor accumulation of FMT and FDG, ROIs 1 cm in diameter were manually placed on the SUV images over the area corresponding to the lesions, which included the site of maximal FMT or FDG accumulation.

Tumor-to-normal cortex count (T/N) ratio and tumor-to-white matter count (T/W) ratio were also determined on the attenuation-corrected FMT and FDG PET images. Counts in tumor, normal cortex and white matter were calculated from ROIs defined in the same way as those used on SUV images. If the tumor was localized in the centrum semiovale, ROIs of cortex and white matter were defined on the contralateral site.

Statistical Analysis

The relationship between FMT and FDG SUVs in the lesions was assessed by linear regression analysis. The differences in mean SUV, mean T/N ratio and mean T/W ratio of FMT among histologic grades, and in mean SUV, mean T/N ratio and mean T/W ratio between FMT and FDG in lesions were evaluated for statistical significance with nonparametric Mann-Whitney test. $P < 0.05$ was considered significant.

RESULTS

Radiosynthesis of FMT was completed within 45 min after the end of bombardment of ^{18}F-fluoride. The mean radiochemical yield of FMT was 20% with respect to the

trapped $CH_3COO^{18}F$, and the mean radiochemical purity of the final solution was >95%.

Approximately 1480 MBq (40 mCi) FMT were produced in one radiosynthesis. In 11 healthy volunteers, no adverse reactions were observed after intravenous injection of FMT.

The average percentage of unmetabolized FMT in the plasma at 5, 30 and 60 min postinjection was 73%, 75% and 78%, respectively (n = 3). The average percentage of unmetabolized FMT in the urine at 60 min postinjection was 86.6% (n = 3).

Intense uptake of FMT was observed only in urinary bladder, and its faint uptake was shown in brain, kidney and liver. The total uptake in brain of FMT, as determined by whole-body scan in 3 healthy volunteers, was 2.8%, 3.9% and 4.9% of injected dose at 30 min, respectively. Free radioactive fluoride was less than 0.5% of total radioactivity at 5, 30 and 60 min postinjection. The amount of urinary excretion of FMT was 46%, 48% and 50%, for the first 60 min and 21%, 22% and 25% for the subsequent 2 h, respectively. The radiation dose to the whole body in 3 healthy volunteers was estimated at 0.049, 0.048 and 0.041 mSv/MBq, respectively.

FMT in blood disappeared rapidly with a $t_{1/2}$ of about 3 min (Fig. 1). In healthy volunteers, rapid incorporation of FMT into the brain tissue and maximal brain uptake of FMT between 15 and 25 min postinjection were observed. This was followed by a washout phenomenon (Fig. 1). Brain images of FMT PET revealed faint cortical uptake (Fig. 2), and the cortical SUV of FMT at 30 min postinjection in 8 healthy volunteers (including 4 healthy volunteers who underwent dynamic scanning) ranged from 1.3 to 2.3 with a mean value of 1.61 ± 0.32.

FMT was rapidly incorporated into a brain tumor to reach the maximal count level at about 10 min postinjection and remained in the brain tumor until 30 min postinjection (Fig. 3). All 23 FMT PET studies in 20 patients (3 patients underwent FMT PET twice) clearly detected the brain tumors (Figs. 4–6).

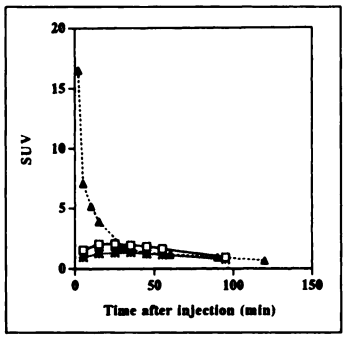

FIGURE 1. Plasma clearance of FMT and time course of FMT uptake in brain. Plasma radioactivity (▲) rapidly decreased after intravenous administration, and its $t_{1/2}$ was about 3 min. In 4 healthy volunteers who underwent dynamic scanning for 100 min, brain FMT uptake rapidly increased after injection reaching maximal value between 15 and 25 min postinjection. After 25 min postinjection, brain FMT uptake decreased gradually with time. Cortical FMT uptake (□) was significantly higher than white matter (*) ($P < 0.01$). Each point is expressed as mean value of 4 healthy volunteers.

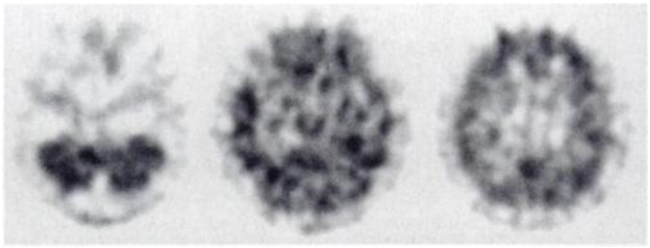

FIGURE 2. FMT PET image of brain in healthy volunteer. Cross sections of cerebellum (left), basal ganglia (middle) and centrum semiovale (right). Faint cortical uptake was observed on FMT PET image obtained at 30 min postinjection.

Tumor SUV of FMT ranged from 1.2 to 8.2 with a mean value of 2.83 ± 1.57 (n = 23), which was significantly higher than cortical SUV of FMT in healthy volunteers ($P < 0.01$). T/N and T/W ratios of FMT ranged from 0.96 to 6.03 with a mean value of 2.29 ± 1.13 (n = 23) and ranged from 1.58 to 8.63 with a mean value of 3.51 ± 1.89 (n = 23), respectively. There was no significant difference of tumor SUV, T/N ratio and T/W ratio between low-grade and high-grade glioma (astrocytic tumors in Table 1) (2.78 ± 1.53 [n = 8] versus 2.60 ± 0.27 [n = 5] in tumor SUV, 2.10 ± 0.82 versus 3.43 ± 1.63 in T/N ratio, 3.61 ± 1.70 versus 4.84 ± 2.70 in T/W ratio). In 3 patients with low-grade glioma, CT or MR images revealed no contrast enhancement (patients 2, 4 and 15); however, the tumor SUV of FMT was higher than 2.0.

In 13 patients, FDG PET scans were obtained within 1 wk of FMT PET studies. T/N and T/W ratios of FMT values were significantly higher than those of FDG PET (2.53 ± 1.31 versus 1.32 ± 1.46, $P < 0.001$; 3.99 ± 2.10 versus 1.39 ± 0.65, $P < 0.0001$, respectively). In 9 of 13 patients, tumor SUVs of FDG could be determined. In the other 4 patients, tumor SUVs of FDG could not be assessed because of technical problems. There was no significant difference between tumor SUV of FMT and that of FDG (3.73 ± 2.25 versus 4.58 ± 2.48 [n = 9]), and there was also no significant correlation between the two.

DISCUSSION

In this study, we could attain sufficient radioactivity level of approximately 1480 MBq (40 mCi) FMT by one radiosynthesis, making it possible to conduct PET studies in 4

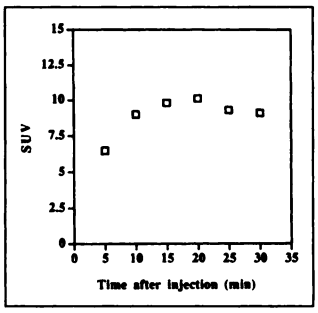

FIGURE 3. Time course of tumor SUV of FMT in patient with brain tumor. Data were expressed as SUV of tumor in patient with astrocytic tumor grade III (patient 10). Tumor SUV of FMT reached its maximum level at about 10 min postinjection and remained at that level for 20 min.

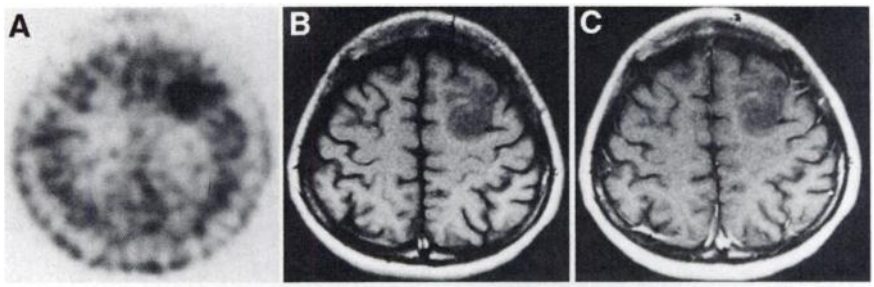

FIGURE 4. 34-y-old woman with astrocytic tumor grade II who suffered from epilepsy (patient 2). (A) FMT PET image obtained at 30 min postinjection reveals intense uptake in brain tumor with SUV of 2.5. T1-weighted MR images without (B) and with (C) contrast media demonstrate tumor as low-intensity mass (B), and no contrast enhancement was observed. After PET scan, tumor was removed surgically and histopathologically proven to be astrocytic tumor grade II.

patients. The chemical yield of FMT was close to that of FDG, which used ^{18}F produced by a $^{20}Ne(d,\alpha)^{18}F$ reaction (*26*), but lower than that of FDG, which used ^{18}F produced by an $^{18}O(p,n)^{18}F$ reaction (*27*). A more efficient radiosynthesis of FMT has to be developed if FMT is to be shared by other medical institutions.

Blood and urine analysis revealed that about 75% radioactivity remained in the unmetabolized FMT. This finding indicates that in vivo stability of FMT is characteristic of humans as well as animals (*20*). The biodistribution in the whole body, total uptake of brain and the amount of urinary excretion of FMT seemed to be similar to those of IMT (*18*). Although the radiation dose to the whole body of FMT (0.041–0.049 mSv/MBq) was higher than that of FDG (0.024 mSv/MBq)(*28*) and ^{123}I-IMT (0.007 mSv/MBq) (*18*), this was a preliminary result in only 3 healthy volunteers. Further investigation of volunteers is needed for the estimation of absorbed doses in humans as a result of intravenous administration of FMT.

Rapid uptake in brain tissue and brain tumors observed in this study corresponded well with the results of fundamental experiments that used tumor-bearing animals (*20,21*).

FMT might be incorporated into the tumor cell by active amino acid transport system as well as the other metabolic tracer of amino acid such as ^{11}C-MET, ^{18}F-tyrosine, ^{11}C-tyrosine and IMT (*9,10,15,19,20,29–31*). Only an insignificant amount of FMT can be metabolized in the tumor cell such as IMT (*18,20*). Although quantitative analysis of FMT in brain tumor based on the dynamic PET images and the data of multiple arterial blood sampling was not performed in this study, the simple metabolic fate of FMT suggests that basic kinetic model may be applied as one-compartment analysis (*30*).

FMT PET detected all 23 brain tumors clearly (Table 1, Figs. 4–6), because the physiological cortical uptake around the tumor was lower than FDG. Breakdown of the blood-brain barrier does not seem to be a prerequisite for FMT tumor uptake because large neutral amino acids enter normal brain tissue. In fact, the intense tumor uptakes on FMT PET images were observed in low-grade gliomas that showed no contrast enhancement on CT or MR images, indicating an intact blood-brain barrier. Recently, Langen et al. (*31*) reported that imaging of tumor extent with IMT SPECT was comparable with ^{11}C-MET PET. Even if tumor SUVs of FMT are not higher than those of FDG, high-contrast tumor images produced by an FMT brain PET scan make it a more desirable clinical procedure for detecting brain tumors than FDG brain PET scans. On the other hand, a faint FMT uptake in normal brain tissue may help us to localize a tumor in the brain, as shown on IMT SPECT and ^{11}C-MET PET.

A significant correlation of tumor uptake and histologic grade in patients with glioma was reported with FDG and

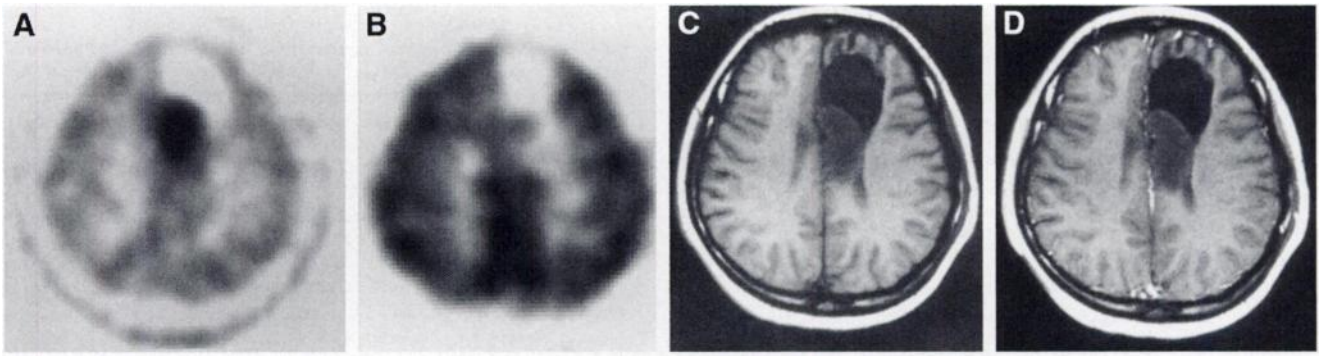

FIGURE 5. 32-y-old woman with recurrent astrocytic tumor grade II (patient 6). (A) FMT PET image obtained at 30 min postinjection demonstrates higher tumor uptake with SUV of 2.5, whereas (B) FDG PET image obtained at 50 min postinjection shows partial tumor uptake. T1-weighted MR images obtained without (C) and with (D) contrast media reveal low-intensity mass with minimal contrast enhancement. Comparing surgical findings, tumor extent demonstrated on FMT PET image was more accurate than that on FDG PET image.

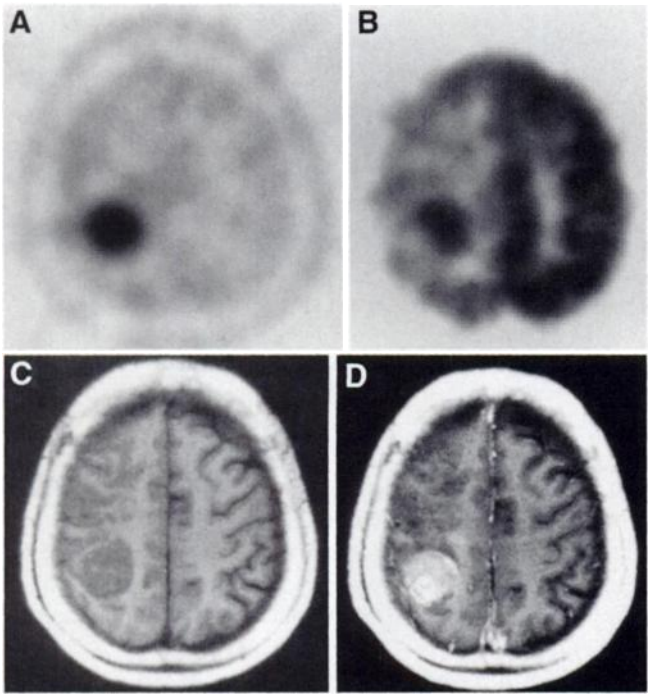

FIGURE 6. 60-y-old woman with astrocytic tumor grade III (patient 10). (A) FMT PET image obtained at 30 min postinjection shows intense tumor uptake of SUV 8.2. (B) FDG PET image obtained at 50 min postinjection also demonstrates hypermetabolic tumor of SUV 9.9 associated with inhibition of glucose metabolism surrounding lesion. Markedly enhanced lesion was recognized on T1-weighted MR images obtained without (C) and with (D) contrast media.

^{201}Tl (*32,33*). The relationship of tumor IMT uptake and histologic grading or FDG uptake of glioma is still controversial (*34–36*). Although further investigation of FMT uptake in glioma is needed, the tumor uptake of FMT seems to be independent of histologic grades of glioma and of the tumor uptake of FDG because clear tumor uptake of FMT was also observed in patients with astrocytic tumor grade II showing low FDG uptake (Figs. 4 and 5). Similar findings have been described with ^{11}C-MET in glioma patients (*1*). On the basis of these characteristics of FMT as a marker of amino acid transport, FMT PET might be an effective technique for assessing the extent of brain tumor and also be useful for preoperative planning of tumor resection and delineating the irradiation field (*34*). Although CT and MRI are unsurpassed diagnostic modalities for the detection of brain tumors, they are limited in the differentiation of tumor tissue from edematous and necrotic tissue.

Although clinical usefulness of IMT SPECT in patients with brain tumors is not contested (*34–37*), FMT PET has some advantages over IMT SPECT. In general, radioiodinated compounds are not adequately stable because of in vivo deiodination. For IMT, in vivo deiodination within the first hour is minimal, but it is metabolized and after 90 min only 30% of IMT remains as an intact tracer (*18*). In contrast, approximately 75% of FMT in the plasma remains in the intact form for 60 min. Fluorinated compounds are stable in vivo, because little ^{18}F-fluoride was detected in animals (*20*) and in healthy volunteers injected with FMT in this study, and no obvious skull uptake was observed in volunteers and patients with brain tumors (Figs. 2, 4–6) as a result of released free ^{18}F. Circular radioactivity outside the brain shown on the FMT PET image seemed to be the uptake in melanocyte in the hair root. Lower FMT uptake in the frontal region than that in the temporal and occipital regions was observed. This corresponded to the density of the hair root. If it is a bony uptake in skull, ringlike radioactivity should be seen, even around the brain. This can also be an uptake in the soft tissue of the scalp, as it is usually seen with other amino acids. However, the time course of FMT in this area seemed to be similar to that of tumors (data not presented). IMT also has a high affinity to melanoma (*38,39*). In spatial resolution for tumor detection and quantification of tumor metabolism, PET is superior to SPECT. In addition, new technology such as the gamma camera with 511-Kev collimator or coincidence circuit may facilitate imaging with ^{18}F-labeled compounds (*40,41*).

CONCLUSION

FMT, like other radiolabeled amino acids, can provide high-contrast images and may have clinical application.

ACKNOWLEDGMENTS

We thank the staff at the Department of Neurosurgery, Gunma University School of Medicine, for their clinical support. We also thank Kunio Matsubara, Saleh Alyafei, Hong Zhang and Kazukuni Takahashi for their technological support. This work was presented in part at the Society of Nuclear Medicine's 45th Annual Meeting, Toronto, Canada, 1998.

REFERENCES

1. Ogawa T, Shishido F, Kanno I, et al. Cerebral glioma: evaluation with methionine PET. *Radiology.* 1993;186:45–53.
2. Barrio JR, Keen RE, Ropchan JR, et al. L-[1-^{11}C]leucine: routine synthesis by enzymatic resolution. *J Nucl Med.* 1983;24:515–521.
3. Koeppe RA, Mangner T, Betz AL, et al. Use of [^{11}C]aminocyclohexanecarboxylate for the measurement of amino acid uptake and distribution volume in human brain. *J Cereb Blood Flow Metab.* 1990;10:727–739.
4. Mitsuka S, Diksic M, Takada A, Yamamoto YL. Influence of the tumor mass on the valine rate constants and on valine incorporation into proteins in an experimental brain tumor model. *Neurochem Int.* 1992;20:537–551.
5. Luurtsema G, Medema J, Elsinga PH, Visser GM, Vaalburg W. Robotic synthesis of L-[1-^{11}C]tyrosine. *Appl Radiat Isot.* 1994;45:821–828.
6. Schmall B, Conti PS, Alauddin MM. Synthesis of [^{11}C-methyl]-alpha-aminoisobutyric acid (AIB). *Nucl Med Biol.* 1996;23:263–266.
7. Shinoura N, Nishijima M, Hara T, et al. Brain tumors: detection with C-11 choline PET. *Radiology.* 1997;202:497–503.
8. Hara T, Kosaka N, Shinoura N, Kondo T. PET imaging of brain tumor with [methyl-^{11}C] choline. *J Nucl Med.* 1997;38:842–847.
9. Willemsen ATM, Waarde A, van Paans AMJ, et al. In vivo protein synthesis rate determination in primary or recurrent brain tumors using L-[1-^{11}C]-tyrosine and PET. *J Nucl Med.* 1995;36:411–419.
10. Pruim J, Willemsen ATM, Molennar WM, et al. Brain tumors: L-[^{11}C]-tyrosine PET for visualization and quantitation of the protein synthesis rate. *Radiology.* 1995;197:221–226.
11. Brock CS, Meikle SR, Price P. Does fluorine-18 fluorodeoxyglucose metabolic imaging of tumours benefit oncology? *Eur J Nucl Med.* 1997;24:691–705.

12. Inoue T, Kim EE, Wong FCL, et al. Comparison of fluorine-18-fluorodeoxyglucose and carbon-11-methionine PET in detection of malignant tumors. *J Nucl Med.* 1996;37:1472–1476.
13. Tyler JL, Diksic M, Villemure JG, et al. Metabolic and hemodynamic evaluation of gliomas using positron emission tomography. *J Nucl Med.* 1987;28:1123–1133.
14. Kahn D, Follett KA, Bushnell DL, Nathan MA, et al. Diagnosis of recurrent brain tumor: value of ^{201}Tl SPECT versus ^{18}F-fluorodeoxyglucose PET. *AJR.* 1994;163: 1459–1465.
15. Coenen HH, Kling P, Stöcklin G. Cerebral metabolism of L-[2-^{18}F]fluorotyrosine: a new PET tracer of protein synthesis. *J Nucl Med.* 1989;30:1367–1372.
16. Kubota K, Ishiwata K, Kubota R, et al. Feasibility of fluorine-18-fluorophenylalanine for tumor imaging compared with carbon-11-L-methionine. *J Nucl Med.* 1996;37:320–325.
17. Tomiyoshi K, Amed K, Muhammad S, et al. Synthesis of new fluorine-18 labeled amino acid radiopharmaceutical: L-^{18}F-alpha-methyl tyrosine using separation and purification system. *Nucl Med Commun.* 1997;18:169–175.
18. Langen KJ, Coenen HH, Roosen N, et al. SPECT studies of brain tumors with L-3-[^{123}I]iodo-α-methyl tyrosine: comparison with PET, ^{124}IMT, and first clinical results. *J Nucl Med.* 1990;31:281–286.
19. Langen KJ, Roosen N, Coenen HH, et al. Brain and brain tumor uptake of L-3-[^{123}I]iodo-α-methyl tyrosine: competition with natural L-amino acids. *J Nucl Med.* 1991;32:1225–1228.
20. Inoue T, Tomiyoshi K, Higuchi T, et al. Biodistribution studies on L-3-(^{18}F)fluoro-α-methyl tyrosine: a potential tumor-detecting agent. *J Nucl Med.* 1998;39:663–667.
21. Amano S, Inoue T, Tomiyoshi K, et al. In vivo comparison of radiopharmaceuticals in detecting breast cancer. *J Nucl Med.* 1998;39:1424–1427.
22. Kleihues P, Burger PC, Scheithauer BW. The new WHO classification of brain tumors. *Brain Pathol.* 1993;3:255–268.
23. Hamacher K, Coenen HH, Stocklin G. Efficient stereospecific synthesis of non-carrier-added 2-[^{18}F]-fluoro-2-deoxy-D-glucose using aminopolyether supported nucleophilic substitution. *J Nucl Med.* 1986;27:235–238.
24. Meikle SR, Bailey DL, Hooper PK, et al. Simultaneous emission and transmission measurement for attenuation correction in whole-body PET. *J Nucl Med.* 1995;36:1680–1688.
25. Syder WS, Ford MR, Warner GG, Watson SS. "S," absorbed dose per unit cumulated activity for selected radionuclides and organs. *MIRD Pamphlet No. 11.* New York, NY: Society of Nuclear Medicine; 1975.
26. Diksic M, Jolly D. New high-yield synthesis of ^{18}F-labelled 2-deoxy-2-fluoro-D-glucose. *Int J Appl Radiat Isot.* 1983;34:893–896.
27. Kleck JH, Benedict SH, Cook JS, Birdsall RL, Satyamurthy N. Assessment of ^{18}F gaseous releases during the production of ^{18}F-fluorodeoxyglucose. *Health Phys.* 1991;60:657–660.
28. Mejia AA, Nakamura T, Masatoshi I, Hatazawa J, Masaki M, Watanuki S. Estimation of absorbed doses in humans due to intravenous administration of fluorine-18-fluorodeoxyglucose in PET studies. *J Nucl Med.* 1991;32:699–706.
29. Kawai K, Fujibayashi Y, Saji H, et al. A strategy for the study of cerebral amino acid transport using iodine-123-labeled amino acid radiopharmaceutical: 3-iodo-alpha-methyl-L-tyrosine. *J Nucl Med.* 1991;32:819–824.
30. Kawai K, Fujibayashi Y, Yonekura Y, et al. Canine SPECT studies for cerebral amino acid transport by means of ^{123}I-3-iodo-α-methyl-L-tyrosine and preliminary kinetic analysis. *Ann Nucl Med.* 1995;9:47–50.
31. Langen KJ, Ziemons K, Kiwit JCW, et al. 3-[^{123}I]Iodo-α-menthyltyrosine and [methyl-^{11}C]-L-methionine uptake in cerebral gliomas: a comparative study using SPECT and PET. *J Nucl Med.* 1997;38:517–522.
32. Di Chiro G, De LaPax RL, et al. Glucose utilization of cerebral gliomas measured by [^{18}F]fluorodeoxyglucose and positron emission tomography. *Neurology.* 1982; 32:1323–1329.
33. Oriuchi N, Tomiyoshi K, Inoue T, et al. Independent thallium-201 accumulation and fluorine-18-fluorodeoxyglucose metabolism in glioma. *J Nucl Med.* 1996;37: 457–462.
34. Weber W, Bartenstein P, Gross MW, et al. Fluorine-18-FDG PET and iodine-123-IMT SPECT in the evaluation of brain tumors. *J Nucl Med.* 1997;38:802–808.
35. Woesler B, Kuwert T, Morgenroth C, et al. Non-invasive grading of primary brain tumors: results of a comparative study between SPECT with ^{123}I-a-methyl tyrosine and PET with ^{18}F-deoxyglucose. *Eur J Nucl Med.* 1997;24:428–434.
36. Kuwert T, Probst-Cousin S, Woesler B, et al. Iodine-123-α−methyl tyrosine in gliomas: correlation with cellular density and proliferative activity. *J Nucl Med.* 1997;38:1551–1555.
37. Kuwert T, Woesler B, Morgenroth C, et al. Diagnosis of recurrent glioma with SPECT and iodine-123-α-methyl tyrosine. *J Nucl Med.* 1998;39:23–27.
38. Bockslaff H, Kloster G, Stöcklin G, Safi N, Bornemann H. Studies on L-3-^{123}iodo-α-methyl-tyrosine: a new potential melanoma seeking compound. *Nuklearmedizin.* 1980;(suppl 17):179–182.
39. Bockslaff H, Kloster G, Dausch D, Schad K, Hundeshagen H, Stöcklin G. First clinical results using L-3-^{123}I-α-methyltyrosine for the non-invasive detection of intraocular melanomas. *Nuklearmedizin.* 1981;(suppl 18):840–844.
40. Martin WH, Delbeke D, Patton JA, Sandler MP. Detection of malignancies with SPECT versus PET, with 2-[fluorine-18]fluoro2-deoxy-D-glucose. *Radiology.* 1996;198:225–231.
41. Jarritt PH, Acton PD. PET imaging using gamma camera systems: a review. *Nucl Med Commun.* 1996;17:758–766.